ANL-76-51

STUDIES OF UNPROTECTED LOSS-OF-FLOW ACCIDENTS FOR THE CLINCH RIVER BREEDER REACTOR

by

H. H. Hummel, P. A. Pizzica,
and Kalimullah

U of C-AUA-USERDA

ARGONNE NATIONAL LABORATORY, ARGONNE, ILLINOIS

Prepared for the U. S. NUCLEAR REGULATORY COMMISSION
under Contract W-31-109-Eng-38

Printed in the United States of America
Available from
National Technical Information Service
U. S. Department of Commerce
5285 Port Royal Road
Springfield, Virginia 22161
Price: Printed Copy $4.00; Microfiche $2.25

Distribution Category:
Advanced Reactor Safety Research-
Fast Reactors (NRC-7)

ANL-76-51

ARGONNE NATIONAL LABORATORY
9700 South Cass Avenue
Argonne, Illinois 60439

STUDIES OF UNPROTECTED LOSS-OF-FLOW ACCIDENTS FOR THE CLINCH RIVER BREEDER REACTOR

by

H. H. Hummel, P. A. Pizzica,
and Kalimullah

Applied Physics Division

April 1976

Work performed for the
Division of Reactor Safety Research

TABLE OF CONTENTS

LIST OF FIGURES

LIST OF TABLES

ABSTRACT

Studies of unprotected loss-of-flow accidents in the CRBR for various rates of flow coastdown and with various options in the SAS 3A code did not lead to conditions for a violent disassembly. Maximum fuel temperatures using the SLUMPY module for disassembly were in the range 4000-4500°C. An approximate treatment of the LOF-driven TOP accident, not properly modeled by SAS 3A, indicates the possibility of some increase in accident severity. The effect of fission gas in dispersing fuel was not taken into account in these calculations. Parameter variations included the presence or absence of axial fuel expansion and of clad motion and use of the moving coolant film model versus the static film model. Study of severe pipe rupture accidents with scram indicated that pin power density and fuel-clad conductance were important parameters in determining what coolant flow rate was needed to prevent boiling after the rupture. It appears that for the CRBR when engineering hot channel factors are considered, this fraction would have to exceed 25%.

I. INTRODUCTION

Although hypothetical core disruptive accidents (HCDA's) in LMFBR's are regarded as very unlikely, there have been and are continuing to be extensive studies of what the consequences of such events might be, in order to assure that any hazard to the public from operation of LMFBR's is of negligible probability. The present paper is concerned with studies of accidents initiated in the Clinch River Breeder Reactor (CRBR)[1] by a loss of sodium coolant flow (LOF) coupled with a failure to scram, leading to possible sodium boiling and voiding, clad melting, and eventual fuel melting and vaporization. Such accidents could result from a loss of electrical power to the primary sodium pumps, or, regarded as much less likely, a massive primary pipe rupture. The purpose of the present series of calculations is to gain understanding of accident characteristics and to study the limitations of available computational tools for accident calculations. Although LOF accidents are not the only ones that have been considered for LMFBR's, they lead to a sufficiently wide range of phenomena to give considerable insight into the behavior of HCDA's, and their consequences are usually found to bound those of other accidents.

II. PHYSICAL MODEL OF THE CRBR

The characteristics of the current design of the CRBR are detailed in the Preliminary Safety Analysis Report (PSAR).[1] The CRBR has a thermal power of 975 MW, of which about 95% is generated in the core with fresh fuel in the beginning-of-life (BOL) state, with which we shall be mainly concerned here. The core height is 91.44 cm, and the core contains 108 fuel assemblies in the inner enrichment zone and 98 fuel assemblies in the two rows of the outer enrichment zone, plus 19 control and safety rod locations, as shown in Fig. 1. The subassembly pitch at hot, full power conditions is 12.16 cm. For the purpose of LOF calculations with the SAS-3A Code the fuel subassemblies have been grouped as shown in Table I into 10 channels, for each of which SAS performs calculations for a single fuel pin representing all the pins in the subassemblies in the given channel. The power distribution in this table was based on 2D triangular mesh calculations.

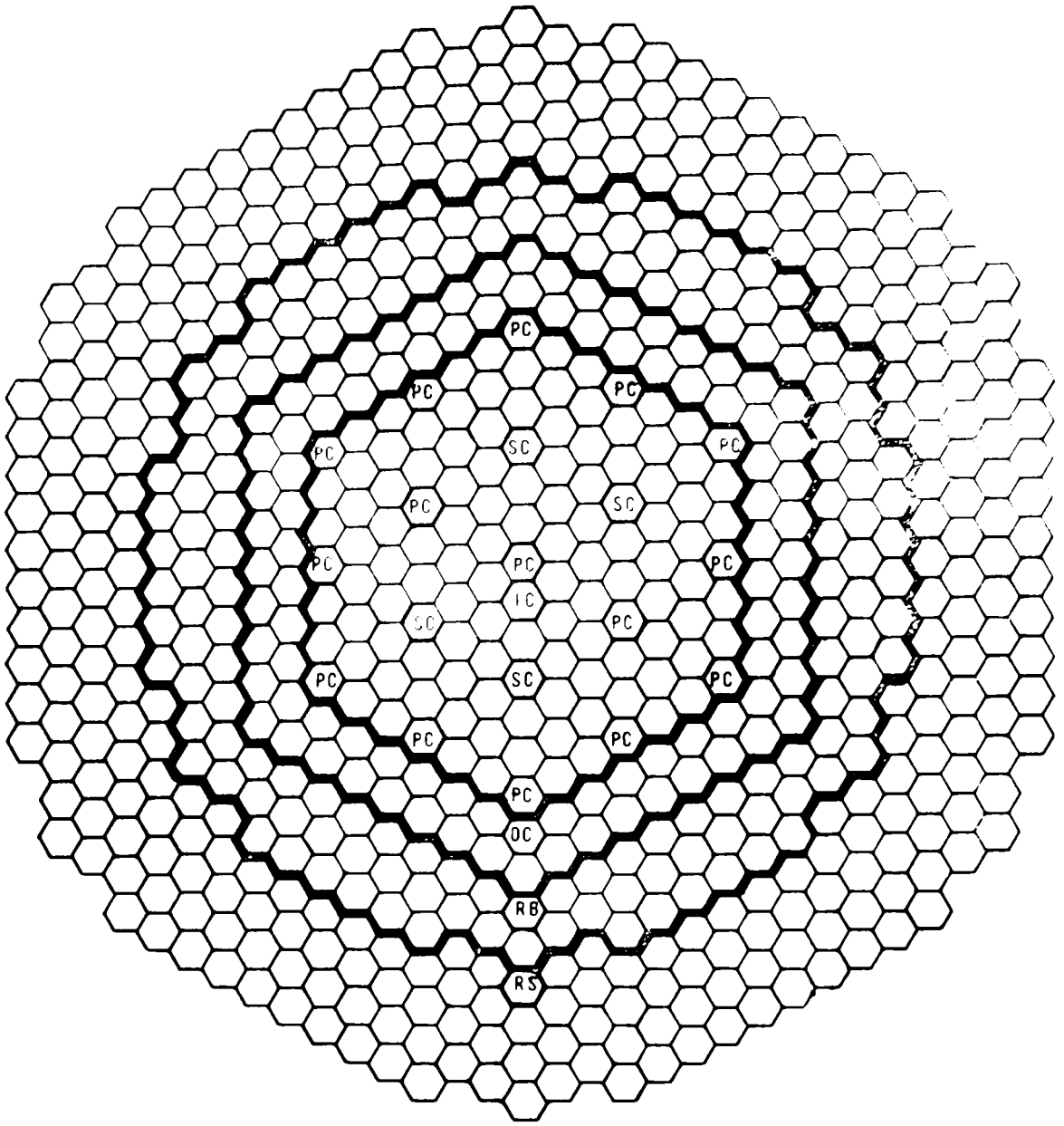

IC - INNER CORE ZONE (108)
OC - OUTER CORE ZONE (90)
RB - RADIAL BLANKET (150)
PC - PRIMARY CONTROL SYSTEM (15 RODS)
SC - SECONDARY CONTROL SYSTEM (4 RODS)
RS - REMOVABLE RADIAL SHIELD (324)

Fig. 1. Reactor Core Cross-section for CRBR.
ANL Neg. No. 116-76-10.

Table I. Ten Channel Model of CRBR

SAS Channel	Number of Subassemblies (Ring)	Relative Radial Power, BOL State	Coolant Mass Velocity, g/cm^2-sec	Relative Power/Flow BOL State	Relative Radial Power, BOEC State	Relative Power/Flow BOEC State
1	6 (2)	1.125	557.8	1.125	1.294	1.294
2	12 (3)	1.191	557.8	1.191	1.238	1.238
3	12 (4)	1.180	557.8	1.180	1.244	1.244
4	24 (5)	1.111	519.1	1.194	1.133	1.217
5	30 (6)	0.996	502.8	1.105	0.977	1.083
6	24 (7)	0.898	437.6	1.144	0.834	1.063
7	24 (8)	1.075	538.4	1.113	1.026	1.063
8	18 (8)	1.062	491.9	1.205	1.026	1.165
9	30 (9)	0.874	438.4	1.112	0.838	1.066
10	18 (9)	0.762	368.1	1.154	0.838	1.270

Reactivity coefficients needed for the SAS-3A code[2] were calculated using an R-Z model of the CRBR shown in Fig. 2. Symmetry about the axial midplane was assumed in these calculations. Partially inserted control rods will cause asymmetries, but the effect of these asymmetries on the overall transient analysis, i.e., on the sequence of events and the conditions at disassembly, is believed to be very small. In any event an R-Z model is rather crude for accounting for control rod effects, and a really satisfactory treatment requires a 3D triangular mesh calculation, not yet feasible for us. For the central control rod and for the 6 control rods on the flats of row 7 uniformly smeared poison corresponding to a 65% insertion of these rods was calculated for criticality. Other control rods were assumed completely withdrawn.

III. CALCULATION OF PHYSICS PARAMETERS

Reactivity coefficients and power distribution for the CRBR were calculated using the ENDF/B-III data in the MC^2-2[3] and SDX[4] codes. Separate cross section sets were generated for inner core and outer core regions, radial blanket, and radial reflector, with sodium both present and voided. Reactivity worths were calculated using first-order perturbation theory, with sodium assumed voided only from within fueled subassemblies. Since the sodium between the subassembly cans and in control rods and control rod channels was not assumed voided, effectively only about two-thirds of the total sodium initially in the core was assumed voided in the flux and adjoint calculations used in obtaining the voided Doppler effect. A 27 group energy structure was used for the cross sections with the first 21 being of uniform 0.5 lethargy from 10 MeV. Values of reactivity coefficients totaled over regions are given in Table II. Details of fuel cycle calculations performed in connection with the equilibrium cycle parameter calculations are given in Ref. 5. The distribution of various physics parameters are shown for the SAS channels in Figs. 3-7 for beginning-of-life (BOL) state for the reactor.

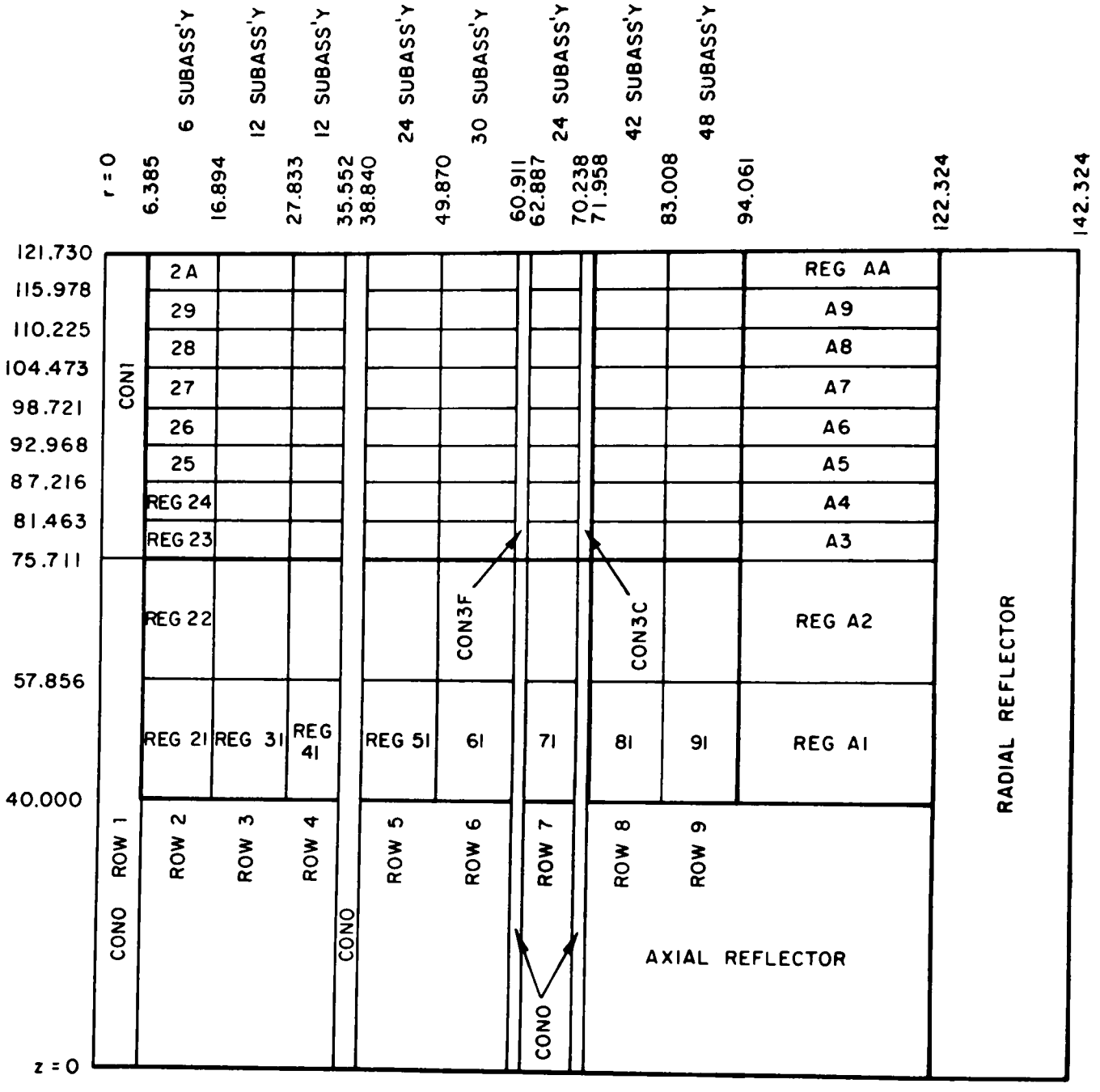

Fig. 2. CRBR, Hot Full Power Dimensions, Lower Half. ANL Neg. No. 116-76-9.

CONO is a collection of spatially disconnected control regions which contain a mixture of sodium and steel representative of the control-rod-out situation.

CON1, CON3F and CON3C are regions representing the central rod, the six rods at flats and the other six at corners of Row 7. These regions contain mixtures of sodium, steel and B_4C representative of the partially inserted rod banks.

REG23, REG24...REG24, REG33...REG7A constitute the inner core;
REG83, REG84...REG8A, REG93...REG9A constitute the outer core and
REGA1, REGA2...REGAA constitute the radial blanket.

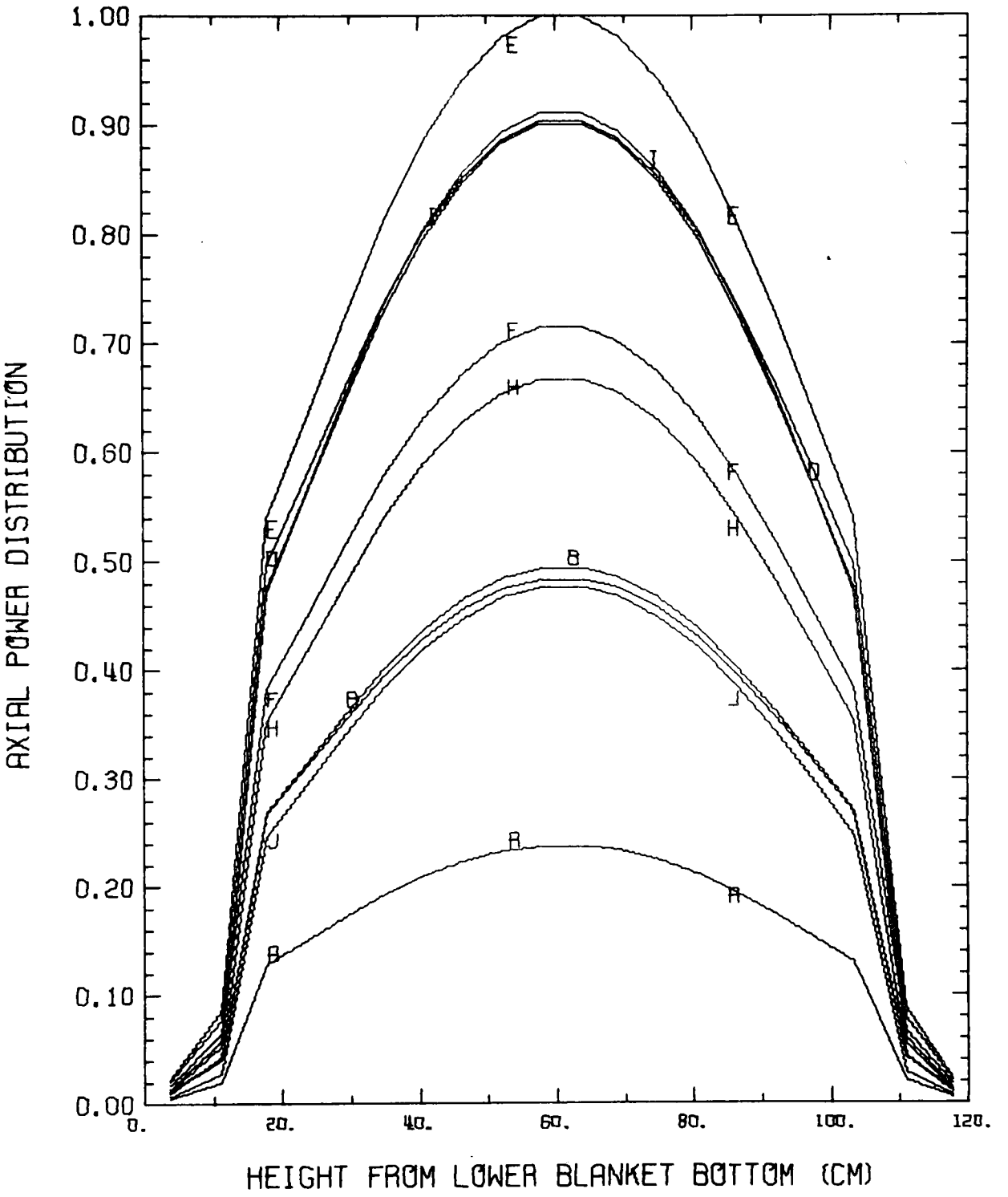

Fig. 3. Axial Power Distribution for CRBR, BOL State. Letters A, B, C, etc. refer to Channels 1, 2, 3, etc. respectively. ANL Neg. No. 116-76-18.

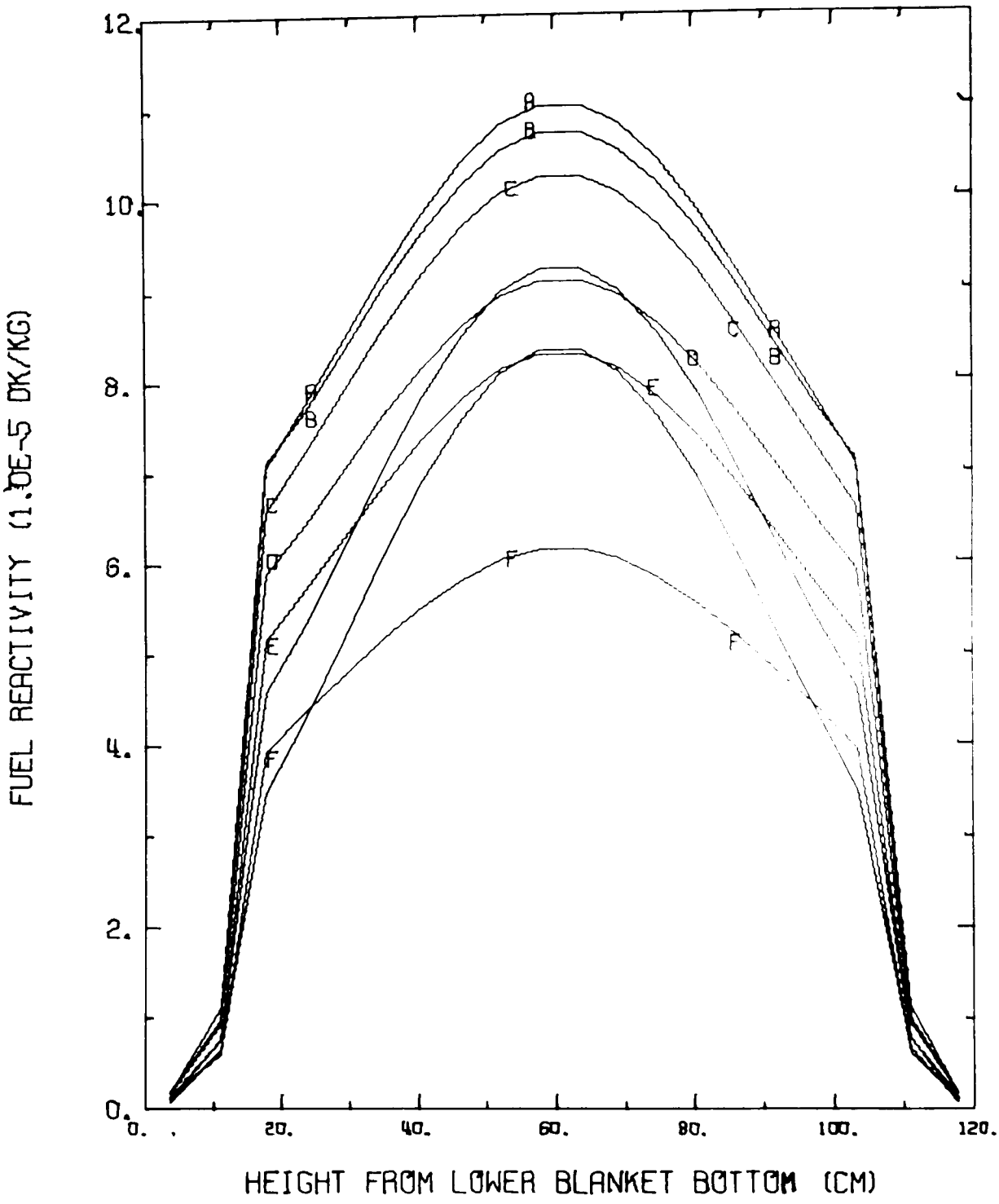

Fig. 4. Fuel Worth for CRBR, BOL State.
ANL Neg. No. 116-76-11.

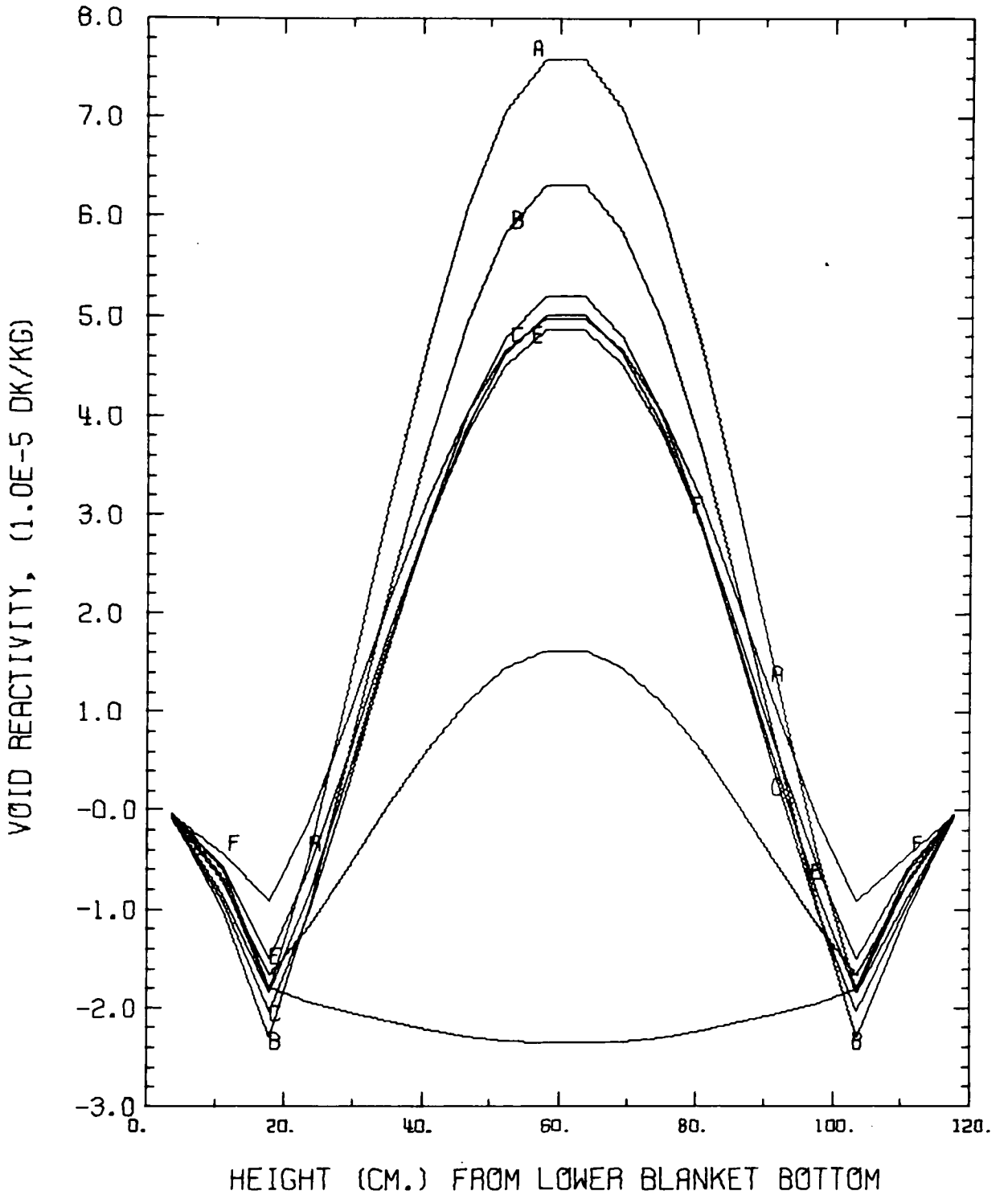

Fig. 5. Sodium Void Worth for CRBR, BOL State.
ANL Neg. No. 116-76-12

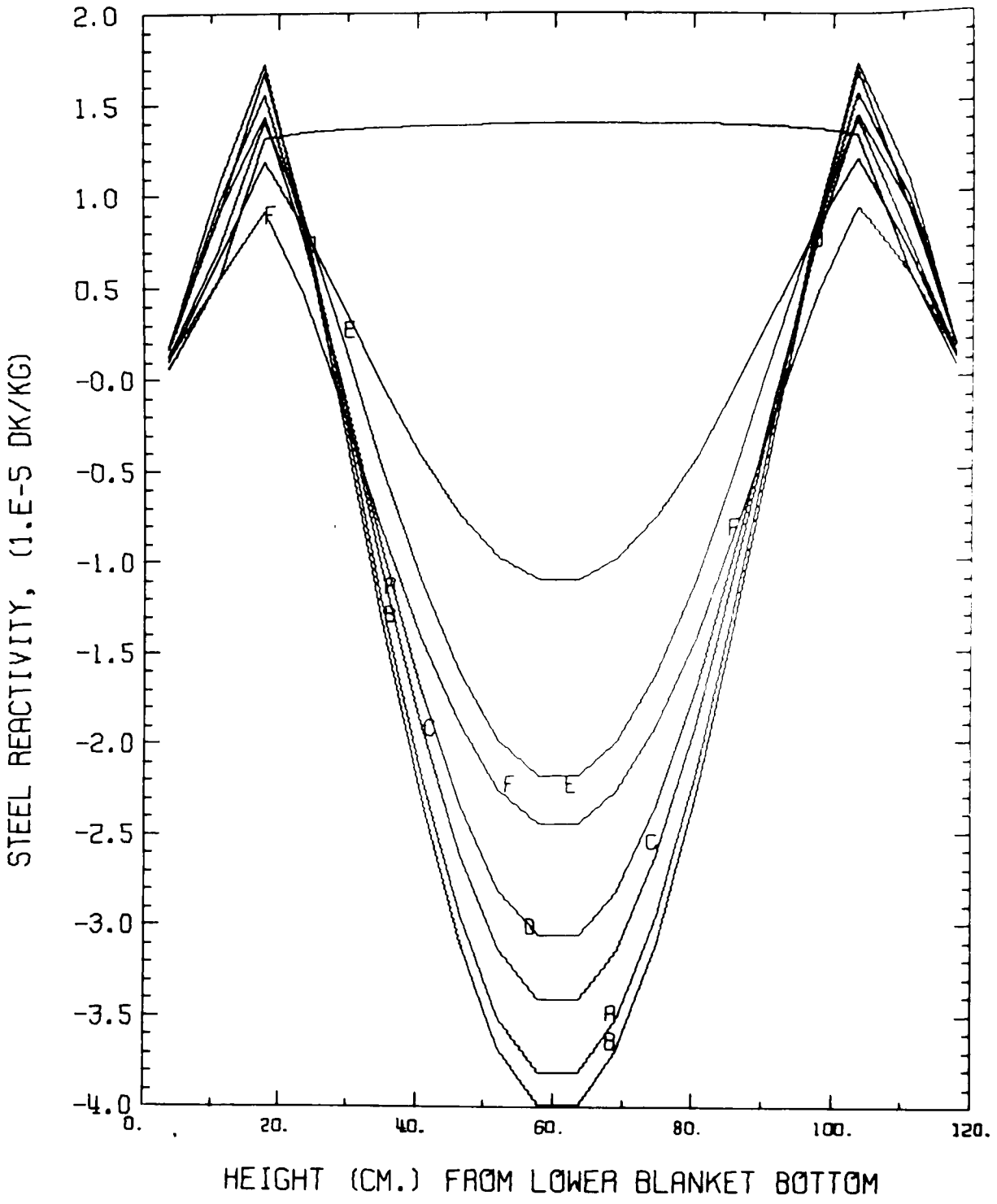

Fig. 6. Clad Worth for CRBR, BOL State.
ANL Neg. No. 116-76-14.

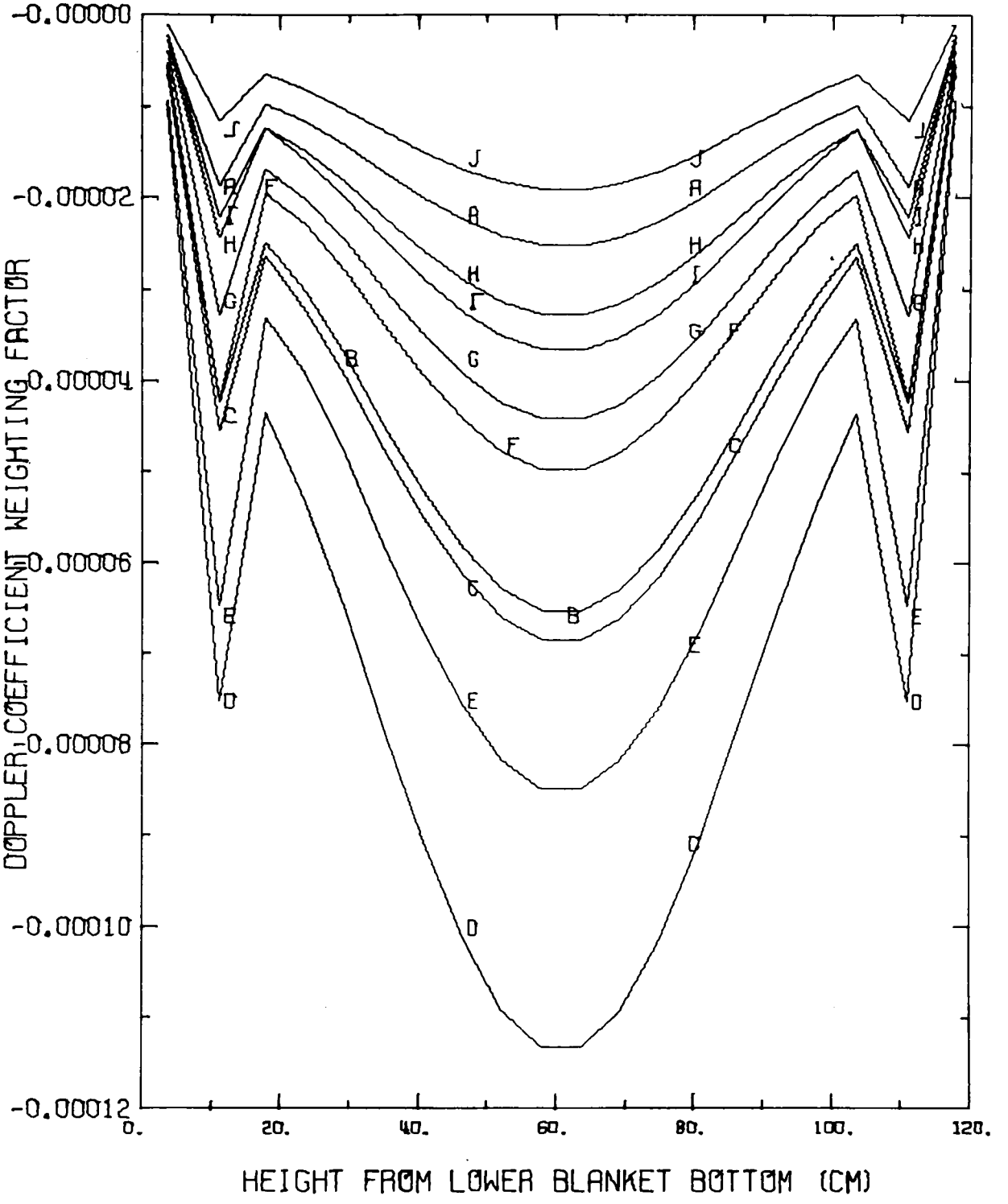

Fig. 7. Doppler Worth Distribution for CRBR, BOL State. ANL Neg. No. 116-76-16.

TABLE II. CRBR Reactivity and Power (RZ Calculation)

	Inner Core	Outer Core	Axial Blankets	Radial Blanket	Total	
Power, MWt	530.6	405.7	13.7	25.0	975.0	BOL
	497.4	369.4	32.7	75.5	975.0	BOEC
	459.8	363.5	52.2	99.5	975.0	EOEC
Sodium Void $\frac{\Delta k}{k} \times 10^3$	9.964	-3.936	-2.373	-1.805	1.850	BOL
	13.200	-0.172	-2.246	-1.516	9.266	BOEC
	14.488	-0.971	-2.544	-1.494	9.480	EOEC
Unvoided Doppler Coeff., $T\frac{dk}{kdT} \times 10^3$	-4.699	-1.511	-0.863	-0.831	-7.904	BOL
	-3.567	-0.955	-1.017	-1.116	-6.655	BOEC
	-3.995	-1.344	-1.352	-1.368	-8.058	EOEC
Voided Doppler Coeff., $T\frac{dk}{kdT} \times 10^3$	-3.282	-1.080	-0.754	-0.769	-5.886	BOL
	-2.457	-0.694	-0.866	-1.038	-5.055	BOEC
	-2.844	-0.964	-1.146	-1.261	-6.214	EOEC

IV. SAS-3A CODE CAPABILITY

Documentation of the SAS-3A code is so far almost entirely in internal ANL reports which have not received wide distribution.[6-11] For an LOF accident this code calculates coolant heating and boiling, clad and fuel heating, melting and motion, and the resultant reactivity feedback effects on the power history, using a point kinetics model. The reactivity effects of fuel axial expansion and structured radial expansion feedback can also be taken into account.

In the boiling process the liquid film on clad and structure may be considered either stationary, or motion of the film through the action of gravity and sodium vapor friction may be taken into account. Calculation of film motion has been found to give a more accurate picture of film dryout and rewetting than the assumption of a static film.[2,10]

Motion of molten clad is calculated by the CLAZAS module of SAS-3A.[8] The resulting reactivity effect has been found to be important for smaller reactors such as the FTR. Clad motion reactivity becomes progressively less important as reactor size increases because prompt criticality, the achievement of which is needed to produce a large power rise and core disassembly, is more readily attained from sodium voiding alone.

When fuel and clad melt and the pin geometry is therefore destroyed, the axial motion of the resulting mixture of fuel, steel, and fission gas is calculated by the SLUMPY module of SAS-3A using compressible hydrodynamics. Slumping of molten fuel under gravity can add reactivity; shutdown occurs eventually from dispersal of core material from fuel or steel vapor pressure or from the action of fission gas. There is no capability for continuing the calculation beyond the limited motion of a first neutronic shutdown. If dispersal of the core material to other parts of the system is blocked by frozen clad and/or fuel, recriticality is a possibility, but this cannot currently be calculated with SAS.

V. PUMP COASTDOWN CALCULATIONS

A. Parameter Studies Performed

1. Introduction

Parameters we have varied in the BOL pump coastdown calculations include the presence or absence of clad motion, the presence or absence of axial expansion, and the use of the sodium film motion model or the static film model.

We have made only very limited SAS calculations for the equilibrium cycle because it appeared in view of the limits of current SAS modeling that not much more useful information would be obtained beyond that gleaned from the BOL studies. We have however, made some parameter studies to scope certain important burnup effects. Fission gas is important in transient overpower (TOP) type pin failures, in which sodium is still flowing and the clad is not yet melted, with clad failure occurring from gas pressure or fuel expansion during the transient. TOP-type failures can occur during a LOF in lower power regions of the reactor, and might contribute important reactivity effects from fuel motion and sodium voiding caused by a molten fuel-coolant interaction (FCI). The SAS-FCI module of SAS-3A[9] was developed to handle TOP-type pin failures, but it is of limited use in a LOF accident because it cannot be applied in channels in which sodium boiling is occurring. SAS-FCI also has other serious defects from a modeling standpoint. An estimate is given later of the possible reactivity effects of pin failures of this type in the CRBR using the PLUTO code,[12] which has a more advanced treatment of the hydrodynamics of the ejection of molten fuel into liquid sodium. PLUTO is a standalone code which does not calculate power generation or heat transfer inside the pin. It can be used to estimate feedback effects which can then be inserted into SAS. Representative amounts of fission gas were assumed in the PLUTO calculations.

Another potentially important effect of fission gas is in dispersing fuel in a disassembly. This could result in final fuel temperatures hundreds of degrees C lower than if generation of fuel vapor pressure is needed, but there is much uncertainty about the effectiveness of fission gas in dispersing fuel and we have not taken it into account. We have, however, studied the effect of a small concentration of fission gas on the rate of fuel slumping in the BOL cases.

A third effect of considering an equilibrium cycle instead of an unburned core is that there is more heterogeneity in the core because of the presence of fuel in various stages of burnup. This will introduce more incoherence into the various reactivity feedback than we have calculated, which will tend to reduce ramp rates somewhat.

The effect of burnup on fuel-clad gap conductance can be important in gas-bonded fuel in its effect on fuel temperature. The significance of gap conductance for pipe rupture accidents is discussed in Section VI.

Finally, for the equilibrium cycle reactivity effects are less favorable than for the BOL state in that the sodium void effect is 30-40% more positive and the Doppler coefficient is lower by 20-30%, as seen in Table II. Limited calculations with beginning-of-equilibrium cycle (BOFC) reactivity coefficients, described below in Section V.A.7, did not however result in an increase in accident severity.

2. Effect of Sodium Film Motion

All the calculations presented in this report used the static sodium film model unless the use of the film motion model is specifically indicated. In Tables III, IV, and V it is seen that the effect of sodium film motion on the results is not large. Comparison of the corresponding core with a static film assumed indicates a time delay of 0.1 sec or less in the start of clad and fuel motion with the film motion model, because of the greater tendency for rewetting of the dried-out clad. The ultimate consequences of the differences between the two models as far as disassembly conditions are concerned are inconsequential, however, as is seen in Table V. Further comparisons of the moving and static film models are given in Section VI.

3. Effect of Clad Motion

Clad motion reactivity ramp rates are seen to be larger than those from fuel slumping and from sodium voiding in cases in which clad motion is allowed. There is much uncertainty surrounding clad motion. Fauske[13] has recently hypothesized that because of incoherence effects among the subchannels of a subassembly there will be bypassing of sodium vapor around the region of molten clad, with the result that clad draining under gravity will alternate with levitation by sodium vapor, leaving little net clad motion. Whatever the merits of this hypothesis are, it does seem reasonable that our calculations are giving an upper limit to clad motion effects. SAS not only does not account for intrasubassembly incoherence, but we have also lumped a large number of subassemblies in a single channel, thus not taking account of power and coolant flow rate variations that actually exist among these subassemblies. This incoherence would tend to smooth out variations in the ramp rate and probably lead to lower peak values. In any event, with the present SAS modeling including the use of SLUMPY for disassembly calculations the increase in ramp rate caused by clad motion does not greatly affect the ultimate severity of disassembly as represented by the peak fuel temperature. As long as there is not a large change in ramp rate and a certain amount of prompt negative feedback is available, the introduction of considerable positive and negative effects changes the detailed course of an accident but does not affect its overall severity greatly. There are compensating effects which cause just sufficient reactivity to be introduced to bring the reactor to the vicinity of prompt critical, at which point a power rise introduces negative reactivity feedback, causing this neutronic shutdown. In our calculations this shutdown is caused by motion of fuel under its own vapor pressure.

4. Effect of Axial Expansion

The effect of axial expansion on final fuel temperature is likewise seen to be insignificant. It should be mentioned that the axial expansion reactivity calculated by SAS is much too large because of an error in the formula used, aside from any question of the validity of the physical assumptions involved. It is estimated that the values calculated by SAS should be multiplied by 0.4. Even with this large overestimate the fuel temperature in disassembly is not much affected.

TABLE III. Starting Times for Boiling, Clad Motion, and Fuel Motion[a] for Pump Coastdown Calculations Without Scram

Case	Film Motion No Axial Exp		Static Film No Axial Exp Clad Motion		Static Film Axial Exp Clad Motion		Static Film No Axial Exp No Clad Motion		Static Film Axial Exp No Clad Motion	
Channel	Boiling Time, Sec	Relative[b] Power	Boiling Time, Sec	Relative Power	Boiling Time, Sec	Relative Power	Boiling Time, Sec	Relative Power	Boiling Time, Sec	Relative Power
1	18.937	3.49	18.167	2.97	21.545	3.53	18.133	3.45	21.864	1.29
2	15.716	0.847	15.716	0.847	17.862	0.759	15.715	0.847	17.863	0.759
3	16.030	0.844	16.032	0.843	18.309	0.749	16.048	0.844	18.309	0.749
4	16.120	0.836	16.139	0.835	20.418	0.982	16.131	0.836	20.418	0.982
5	18.335	4.38	18.294	7.12	21.774	2.15	18.230	2.89	22.278	1.03
6	18.341	4.23	18.298	6.17	21.754	2.33	18.231	2.89	22.169	1.14
7	18.274	3.68	18.233	3.08	21.601	2.18	18.159	3.39	22.002	1.12
8	16.030	0.844	16.030	0.843	18.380	0.142	16.026	0.843	18.380	0.742
9	18.440	4.23	18.346	3.95	21.974	1.67	18.348	2.84	23.792	1.48
10	18.455	5.11	18.359	3.87	21.842	1.96	18.366	2.81	23.792	1.48
	Clad Motion Start, Sec	Relative Power	Clad Motion Start, Sec	Relative Power	Clad Motion Start, Sec	Relative Power				
1										
2	18.262	3.51	18.143	3.08	20.797	0.918				
3	18.411	3.19	18.340	4.17	21.217	1.30				
4	18.533	10.7	18.500	18.5						
8	18.542	10.7	18.462	6.70	21.599	2.19				
	Slumping Start, Sec	Relative Power	Fuel Melt Fr	Slumping Start, Sec	Relative Power	Fuel Melt Fr	Slumping Start, Sec	Relative Power	Fuel Melt Fr	Slumping Start, Sec	Relative Power	Fuel Melt Fr	Slumping Start, Sec	Relative Power	Fuel Melt Fr
1															
2	18.570	68.8	0.46	18.523	28.6	0.35	22.409	2.62	0.092	18.923	14.4	0.480	24.560	44.6	0.365
3	18.571	106	0.37	18.538	55.8	0.37	22.514	39	0.292	18.937	26.2	0.470	24.312	22.7	0.354
4	18.573	144	0.33	18.542	99.2	0.37	22.562	43	0.33	18.950	43.5	0.459	24.415	22.9	0.315
5													24.536	24.6	0.292
6															
7													24.625	28.6	0.54
8	18.574	158	0.37	18.542	99.2	0.34	22.545	76	0.196	18.950	43.5	0.429	24.566	48.4	0.369
9													24.508	16.6	0.252
10															

[a]Slumping on Clad Melting & Melting of Inner Unrestructured Fuel.

[b]Normalized to Steady-State Power.

Table IV. Fraction of Core Voided of Sodium at Disassembly

Case		1	2	3	4	5
		Film Motion No Axial Exp. Clad Motion	Static Film No Axial Exp. Clad Motion	Static Film Axial Exp. Clad Motion (No Gas)	Static Film No Axial Exp. No Clad Motion	Static Film Axial Exp. No Clad Motion (No Gas)
Time, sec		18.586	18.552	22.612	18.964	24.577
Channel	Sub-assembly	Core Void Fraction	Core Void Fraction	Core Void Fraction	Core Void Fraction	Core Void Fraction
1	6	0.596	0.608	0.805	0.831	0.876
2	12	0.806	1.000	1.000	0.854	0.998
3	12	0.789	1.000	1.000	0.857	0.872
4	24	0.743	0.781	0.984	0.944	1.000
5	30	0.104	0.096	0.540	0.604	0.600
6	24	0.053	0.087	0.310	0.423	0.937
7	24	0.433	0.420	0.653	0.610	0.719
8	18	0.843	0.711	1.000	0.782	0.800
9	30	0.009	0.015	0.0	0.0	0.0
10	18	0.019	0.003	0.0	0.0	0.0
High power Channels 1-4, 7, 8	96	0.689	0.722	0.897	0.801	0.868
Low power Channels 5, 6, 9, 10	102	0.049	0.054	0.232	0.321	0.220

TABLE V. Disassembly Conditions for CRBR Pump Coastdown Calculations Without Scram, BOL State

Case	1	2	3		4		5	
Sodium Film	Moving	Static	Static		Static		Static	
Axial Expansion	No	No	Yes		Yes		No	
Clad Motion	Yes	Yes	Yes		No		No	
Fission Gas	Yes	Yes	Yes	No	Yes	No	Yes	Yes
PLUTO Feedback	No	No	No	No	No	No	No	Yes
Time, Sec	18.579	18.552	22.614	22.609	24.585	24.572	18.978	18.965
Peak Power[a]	266	292	137	177	63	171	305	2930
Max. Temp, °C[b]	4062	4208	4214	4415	4145	4482	4420	5157
Reactivity, $								
Na Voiding	1.285	1.262	1.842	1.867	2.406	2.464	2.149	2.099
Clad Motion	0.901	0.972	2.129	2.136				
Fuel Motion	0.003	0.028	0.869	1.186	1.622	2.113	0.259	0.114
Doppler	-1.183	-1.256	-1.264	-1.378	-1.228	-1.356	-1.406	-1.241
Programmed								0.182
Axial Expansion			-2.576	-2.822	-1.837	-2.213		
Net	1.006	1.005	1.000	0.988	0.963	1.008	1.002	1.155
Ramp Rate, $/sec								
Na Voiding	2.9	1.6	3.6	3.7	5.7	5.8	5.9	10.3
Clad Motion	15.6	15.0	29.1	27.6				
Fuel Motion	2.0	1.9	1.5	8.4	9.4	18.9	16.1	10.8
Programmed								75.0
Total	20.5	18.5	34.2	39.7	15.1	24.7	22.0	96.1

(a) Relative to normal reactor power
(b) For compressible fuel region in SLUMPY.

5. Effect of Ambient Fission Gas on Fuel Slumping

We observed that the drag effect on slumping fuel of ambient fission gas at only several atmospheres pressure was sufficient to reduce the fuel velocity considerably below that of a free fall. In an effort to find an upper limit to the ramp rate that could be produced by fuel slumping, we selected cases in which axial expansion feedback was present to eliminate the fission gas drag effect (cases labeled "no fission gas" in Table V). Some augmentation of the fuel slumping ramp rate was attained in this way, but the maximum ramp rate attained of $19/sec is still moderate. There are limits to how large fuel slumping ramp rates under gravity can be even in the absence of other positive feedbacks.[14] Considering that there will always be a certain amount of fission and fill gas present to exert a drag effect, and that levitation of fuel by fission gas escaping from fuel during a transient may very well occur, it is hard to see how very high fuel slumping ramp rates can occur in an LMFBR.

6. Effect of BOEC Reactivity Coefficients and Power Distribution

Because of the unfavorable variations of reactivity coefficients from the BOL to BOEC state indicated in Table II, a SAS pump coastdown calculation was performed for no axial expansion and no clad motion using the BOEC reactivity coefficients. The same subassembly assignments and coolant velocities as those in Table I for the BOL state were used in these calculations, but an altered power distribution based on a radial model of the CRBR was used (Table I). Results of this calculation are given in Tables VI and VII.

Table VI. Starting Times for Boiling and Fuel Motion for Pump Coastdown Calculations Without Scram for the CRBR With BOEC Reactivity Coefficients, No Clad Motion, No Axial Expansion

	BOL Power Distribution		BOEC Power Distribution	
Channel	Boiling Time, Sec	Relative[a] Power	Boiling Time, Sec	Relative[a] Power
1	15.051	26	12.175	0.968
2	13.424	0.968	12.266	0.967
3	13.686	0.965	13.252	2.02
4	13.728	0.960	13.424	2.39
5	15.076	36	13.931	24
6	15.076	36	13.989	68
7	15.061	27	13.920	16.3
8	13.669	0.966	13.658	3.12
9	15.091	51	13.969	49
10	15.092	53	13.486	2.55

	BOL Power Distribution			BOEC Power Distribution		
Channel	Slumping Time, Sec	Relative Power	Fuel Melt Fraction	Channel	Slumping Time, Sec	Relative Power	Fuel Melt Fraction
2	15.108	50	0.826	1	13.952	38	0.396
3	15.154	48	0.865	2	13.956	36	0.417
8	15.154	46	0.865	3	14.020	91	0.888

[a]Normalized to Steady-State Power.

Table VII. Disassembly Conditions for Pump Coastdown Calculations Without Scram for BOEC Reactivity Coefficient No Axial Expansion, No Clad Motion

Case	BOL Power Distribution	BOEC Power Distribution
Time, Sec	15.164	14.013
Peak Power	222	93
Max. Temp, °C	4375	4093
Reactivity, $		
Na Voiding	2.146	1.876
Fuel Motion	0.077	0.142
Doppler	-1.237	-1.053
Net	0.986	0.965
Ramp Rate, $/sec		
Na Voiding	15	0
Fuel Motion	0	6
Total	15	6

The interesting result was obtained that the disassembly attained was milder than in the corresponding BOL case. Analysis of the results indicated that the effect of increased incoherence resulting from the altered power distribution caused a decrease in ramp rates that outweighed the changes in reactivity coefficients. Also there were compensating effects among feedbacks in that the reduced Doppler coefficient meant that less sodium voiding was needed to attain prompt critical, also tending to reduce the sodium voiding ramp rate. In turn decreased sodium voiding meant that the sodium-in Doppler coefficient applied over more of the core, so that the effective Doppler coefficient was not reduced as much as it otherwise would have been.

In order to separate the effect of power distribution from that of reactivity coefficients a SAS calculation was performed under the same assumptions as the one just described except that the BOL radial power distribution was used. Results are also given in Tables VI and VII. A slightly more severe disassembly was attained comparable to that for the corresponding case using the BOL reactivity coefficients. Compared to that case there was less opportunity for fuel motion reactivity because of the more positive sodium void reactivity addition. Another complicating factor in the case of the BOL power distribution and the BOEC coefficients was that the more rapid power rise associated with more coherence and more positive feedback coefficients caused high fuel melt fractions to be attained before clad melting was complete, a condition required for fuel slumping in our calculation. This may also have acted to reduce fuel motion reactivity effects. Whether this SAS modeling option corresponds to physical reality is an open question since clad failure and fuel motion might very well occur before complete clad melting at high fuel melt fractions.

It appears that because of compensating feedback effects changes in reactivity coefficients of the size found in going from the BOL to the BOEC state are not likely to produce important changes in accident severity.

7. Estimate of Reactivity Effect of LOF-Driven TOP

It is seen in Table IV that, when disassembly conditions are reached in a LOF accident in the CRBR, low power channels have sodium still largely unvoided and the clad is therefore still intact. This is a condition that the present SAS code cannot cope with adequately, as mentioned earlier.

Calculations have been performed with the PLUTO code[12] to try to get a more realistic evaluation of the possible reactivity effects from fuel and sodium motion in the lower-powered channels. If pin failure is assumed to occur at the axial center of the core, motion of molten fuel inside the pin through the clad rip will be toward the center of the core and will add reactivity. Sodium voiding as a result of fuel and fission gas motion through the clad failure will also be positive initially. The effect of a number of variables on the possible reactivity ramp rates has been explored. These variables include pin cavity radius (radius of molten fuel region, in which motion is assumed possible), cavity temperature, cavity fission gas content, and strength of fuel-coolant interaction. Reference values for these variables were assigned on the basis of results in low-powered channels at the time of failure of high-powered channels in an LOF calculation for the CRBR. The reference FCI parameters represent a mild interaction that seems reasonable on the basis of available experiments.[15] Variations of parameters were made over what were considered to be reasonable limits, and conservative values of fuel and sodium ramp rates from TOP-type failures in the low-powered channels were calculated. Coherent failure within a few milliseconds is required if the ramp rate is to be maximized, because after about 10 milliseconds after failure the rate of fuel ejection from the pin caused by the assumed fission gas in the cavity starts to decrease. Examination of the SAS LOF results for the BOL state indicated that such coherence would be a reasonable assumption for 24 subassemblies in Row 7, 18 in Row 8, and 18 in Row 9 of the CRBR, corresponding to SAS channels 6, 8, and 10 in our BOL model. For the equilibrium cycle there should be less coherence than for the BOL state. A conservative estimate of the ramp rate during the first 10 milliseconds after pin failure, assuming these 60 subassemblies to fail coherently, is \$50/second for fuel and \$25/second for sodium (Appendix). The total amount of reactivity added in 50 milliseconds, assuming fuel not to be swept out but to remain in the channel at the point of expulsion, is about \$1 from fuel motion and about \$0.4 from sodium motion. The consequence of a \$75/sec ramp rate at the time of prompt criticality in an SAS calculation is given in Table V. With a total ramp rate of $\sim$100 \$/sec, the maximum fuel temperature is about 5150°C. Use of equilibrium-cycle reactivity coefficients for such a reactivity addition has not been investigated but from the work in the preceding section seems unlikely to make an important difference. Although we have made only a rough estimate of the effect of the LOF-driven TOP, the indication is that it should not be a severe problem in the CRBR.

Once the failure point is assumed to move away from the axial center of the core, reactivity addition rates drop rapidly. For failure 10 cm above the center of the core the fuel reactivity change is only about 40% of that for central failure; for 20 cm above the center the reactivity change becomes negative. For failure below the center of the core fuel sweepout can prolong the time of positive reactivity addition from fuel motion; this has not yet been evaluated in detail. The sodium-reactivity effect for failure 10 cm above the center of the core it is 40-50% of the value for central failure. For failure 10 cm below the center of the core the sodium-reactivity ramp rate is slightly larger than for central failure.

There is a real question about whether the fuel motion inside the pin after failure in these PLUTO calculations is actually physically possible. A considerable amount of fuel melting may be needed before there is much mobility of fuel inside the pin, and by that time fission gas evolution may have caused massive pin failure.[15] In addition, for a LOF accident a large axial region of the pin clad is at nearly the same temperature, so that the concept of a single localized clad failure to which all fuel moves may not be realistic. There is no experimental information on pin failures at high ramp rates with hot clad to indicate what fuel melt fraction can be attained before massive pin failure. For fresh fuel there is certainly a likelihood of high melt fractions, but there is little fission gas available to expel fuel or sodium. Fuel vapor pressure, not accounted for in PLUTO, becomes significant between 3500 and 4000°K.

B. Effect of Modeling of Disassembly Accident Severity

Changes in modeling assumptions or input parameters might lead to more severe disassembly conditions than we have calculated, aside from the possible effect of the LOF-driven TOP. For example, in SLUMPY the pressure generated by the fuel from vapor pressure or fission gas pressure must exceed a specified ambient pressure before any fuel motion occurs. We used the default value of 2.5 atm for this threshold. Setting this pressure at a high value to simulate resistance to fuel movement from structure or solid fuel would increase accident severity. Otherwise only small pressures need to be generated to produce disassembly in the SLUMPY model. Another example of how modeling or input assumptions can affect SLUMPY results is afforded by one of the cases considered in HCDA studies for the CRBR.[16] By making what seems to be a rather improbable combination of assumptions, it is possible to obtain a coherent compaction of the fuel compressible region by vapor pressure of liquid sodium reentering the core from below and contacting hot clad. The resultant reactivity effect elevates the final fuel temperature hundreds of degrees C above what is obtained with the original model.

Another modeling assumption that results in higher final fuel temperatures is to abandon SAS at a given point when the reactor is at or near prompt critical and to continue the calculation with VENUS. It is customary in this procedure to assume that the core is completely voided of sodium which considerably lowers the Doppler coefficient. As a result the final fuel temperature is hundreds of °C higher than it would be if the Doppler coefficient during disassembly was computed more accurately.[16]

VI. PIPE RUPTURE CALCULATIONS

A. Introduction

Prior to the calculation described in Section V, a series of SAS calculations at varying flow rates to simulate the effect of pipe rupture accidents was carried out with a preliminary, somewhat inaccurate model of the BOL state of the CRBR. It is not believed that these inaccuracies in the model made any essential difference in the conclusions reached in the studies in Part B, but do affect those in Part C, which must be regarded as preliminary. Two ranges of coastdown rates were studied. Less severe pipe rupture calculations with

flow decay rates of several seconds were made with scram assumed inoperative. For extreme pipe rupture accidents, in which flow decay occurred in several tenths of a second, calculations were made both with and without scram, but in the latter case the calculation was followed only long enough to estimate when coolant boiling would begin.

B. Less Extreme Pipe Rupture Accidents

Flow reduction rates assumed for the less extreme pipe rupture accidents and also for a pump coastdown calculation carried out with the older model are shown in Fig. 8. The indicated decay periods of 1.5 sec and 4.5 sec are only approximate as the assumed flow decay is not really exponential. Also shown for comparison is the pump coastdown flow reduction curve for the CRBR specified in the PSAR. Results of these calculations are given in Tables VIII and IX.

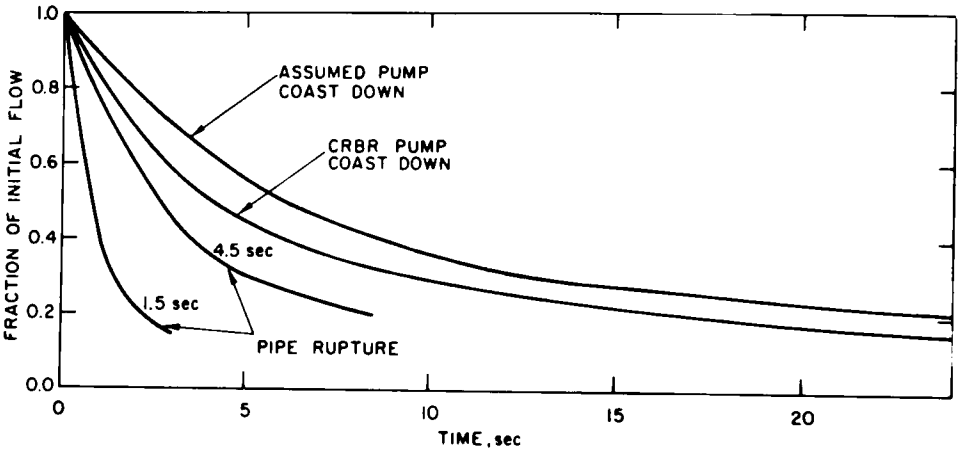

Fig. 8. Flow Reduction Rates for Pump Coastdown and for Less Extreme Pipe Rupture Cases. ANL Neg. No. 116-76-20.

Channels 1, 2, 3, and 7 in this model correspond to subassemblies in rows 2, 3, 4, and part of row 8, and represent regions of higher power or higher power-to-flow ratio. No axial expansion feedback or effect of fission gas in dispersing fuel was assumed in these calculations. It is seen that, while flow coastdown rate affects the time scale of events, it has no significant effect on the severity of disassembly, which is limited as was the case for the calculations in Section V. Fluctuations of ramp rates among various cases are probably not significant as the values of these rates vary with time in the vicinity of prompt critical, due somewhat to the large number of subassemblies grouped in

Table VIII. Starting Times for Sodium Boiling, Clad Motion, and Fuel Motion for LOF Cases Without Scram, Original Reactor Model

Case	Channel	Boiling Time, Sec.	Clad Motion Start, Sec.	Fuel Motion Start, Sec.
Pump Coastdown	1	23.760		25.449
	2	22.743	25.100	25.429
	3	23.263	25.408	25.433
	7	24.653		
4.5 Sec Pipe Rupture	1	8.325		10.120
	2	8.087	10.048	10.102
	3	8.226	10.104	10.104
	7	9.310		
1.5 Sec Pipe Rupture	1	3.089		4.204
	2	2.959	4.171	4.195
	3	3.016	4.184	4.198
	7	3.506		4.244

Table IX. Disassembly Conditions for LOF Cases Without Scram, Original Reactor Model

Case	Pump Coastdown	4.5 Sec Pipe Rupture	1.5 Sec Pipe Rupture
Disassembly Ramp Rates, $/Sec			
Na Voiding	5	10	4
Clad Motion	22	9	16
Fuel Motion	0	2	2
Disassembly Time, Sec.	25.460	10.130	4.247
Max. Fuel Temp, °C	4534	4200	4234
Reactivity Feedback at Prompt Critical, $			
Doppler	-1.288	-1.143	-1.040
Na Void	1.648	1.155	1.831
Clad Motion	0.629	0.366	0.223
Fuel Motion	0.017	0.026	0.011
Net	0.997	1.004	1.025
Na Voiding			
Inner Core	0.64	0.73	0.86
Outer Core	0.14	0.34	0.50

a channel. As with the cases discussed in Section V, ramp rates are calculated to be moderate, with clad motion tending to be predominant over sodium voiding and fuel motion effects being rather small. In these calculations also the possible effect of TOP-type failures in low-power regions has not been taken into account, although the possibility of such events is evident from the large amount of sodium remaining in the core at prompt criticality.

In the case of the 1.5 sec pipe rupture the effect of using the sodium film motion model was investigated. Although the detailed voiding patterns differed in the two cases (Fig. 9 vs. Fig. 10) the times for clad melting was delayed by only 0.1 sec or less because of the greater rewetting of the clad resulting from increased coolant oscillations. According to Höppner,[17] these increased oscillations are due to increased vapor flow resulting from a reduced film thickness on structure (subassembly core wall and wire wrap) in the SAS model. A thick film on structure results from the fact that there is no heat generation in the structure to vaporize the film and action of vapor to strip it off, as happens in the film motion model. In the "two-phase friction factor" option, used in Tables VIII and IX and in Fig. 10, the vapor-film friction factor is enhanced by a multiplier to account for "flooding" of the film, which greatly increases the friction factor. This multiplier is a function of the liquid film thickness, and the result is that the thick film on the structure cases a reduced vapor flow and reduced oscillation of the vapor-liquid interface. This whole effect is rather artificial because the modeling of the structure is crude to begin with, and the thick film on the structure should be swept away by vapor friction, as predicted by the film motion model. A better course in applying the static film model is to elect the option of setting the friction factor multiplier equal to unity. The result of this (Fig. 11) is indeed to increase rewetting of the clad somewhat and to delay the time of clad melting slightly, although the detailed pattern of voiding and rewetting is not the same as for the film motion model. This slight delay in clad wetting had an important consequence in the course of the accident as calculated by SAS-3A both with film motion and with the one-phase friction factor in that the situation arose that the criterion for fuel slumping (in this case melting of the innermost node of the unrestructured fuel) was satisfied before clad melting was complete. (There was only about a 0.02 second delay between clad motion and fuel motion with the two-phase friction factor.) Under these circumstances the SLUMPY module of SAS with the particular input options selected caused clad motion to be suppressed, clad to be mixed with fuel, and sodium vapor to levitate the mixture from the core, causing shutdown with the fuel only at its melting point, 2767°C. This action of sodium vapor is in sharp contrast to the compaction of fuel by sodium vapor pressure obtained with different parameter assumptions mentioned in Section V-C. The physical argument behind this is that, if no clad motion occurs, no blockage of coolant passages by frozen clad will occur, and sweepout of fuel by sodium vapor is reasonable.[18] It seems physically unreasonable that such a short delay in clad melting should influence to this extent whether or not fuel sweepout by sodium vapor should occur, and this aspect of the SAS modeling seems somewhat questionable. A small delay in clad melting reasonably could, however, determine whether or not clad motion occurred before the start of fuel motion, which could have important consequences with respect to reactivity effects and to the possible plugging of coolant passages by frozen clad. Providing a more accurate evaluation of this question may be the most important function of the film motion model.

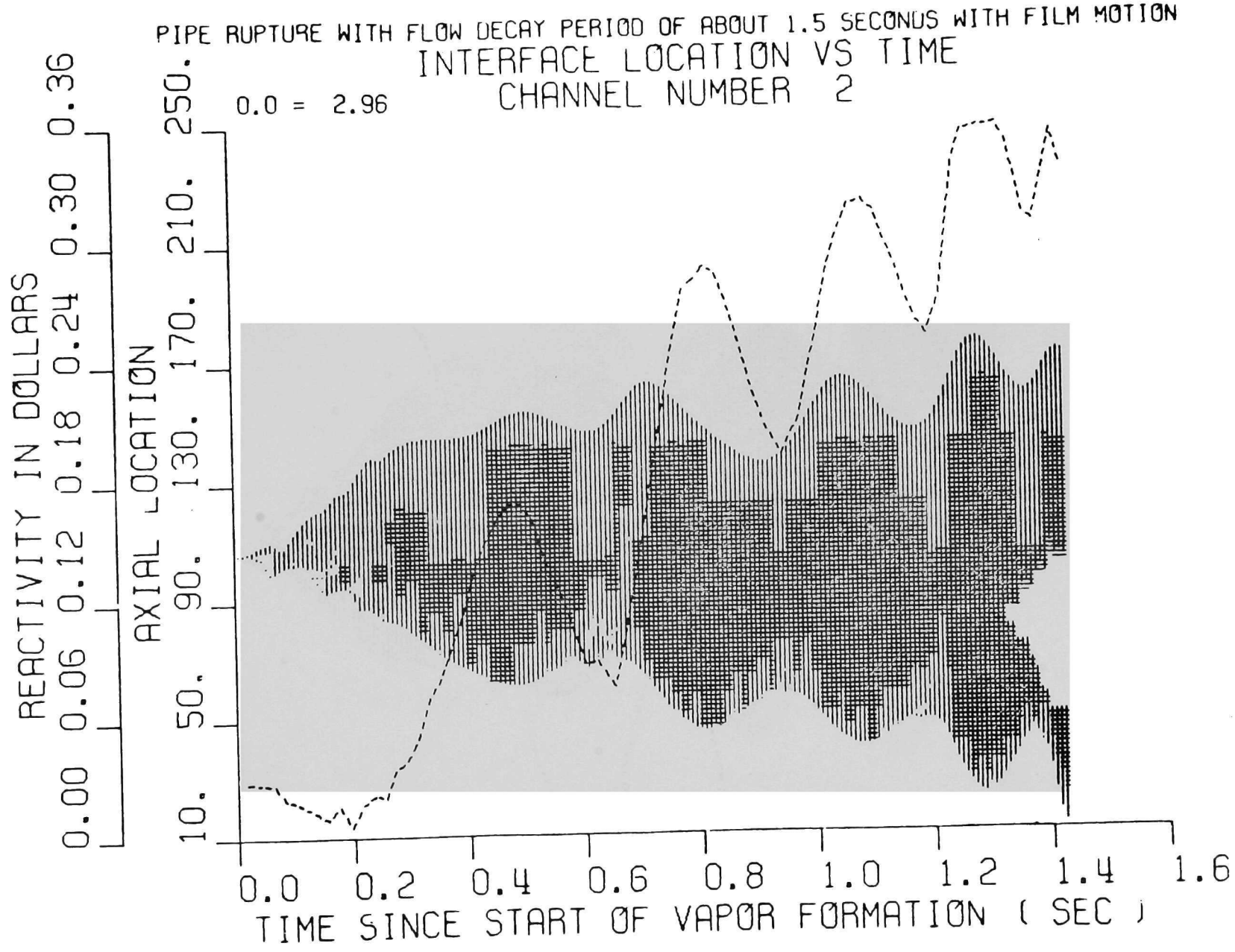

Fig. 9. Sodium Liquid-vapor Interface Location for 1.5 sec Pipe Rupture Accident, Film Motion Option, 2-phase Friction Factor. Cross-hatched areas represent film dryout. Blank area at right represents clad melting. Dashed line gives sodium voiding reactivity. ANL Neg. No. 116-76-17.

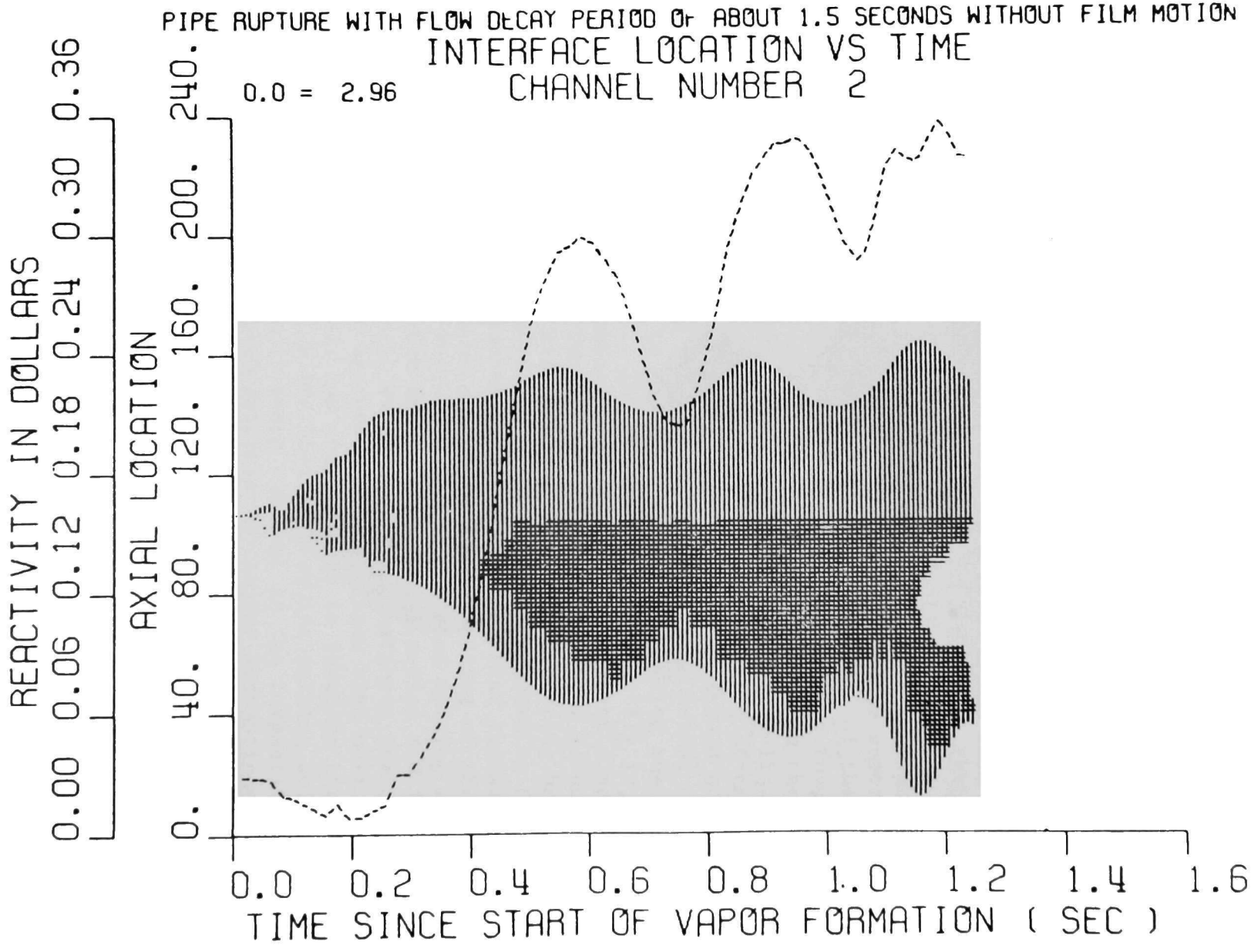

Fig. 10. Sodium Liquid-vapor Interface Location for 1.5 sec Pipe Rupture Accident, Static Film, 2-phase Friction Factor. ANL Neg. No. 116-76-15.

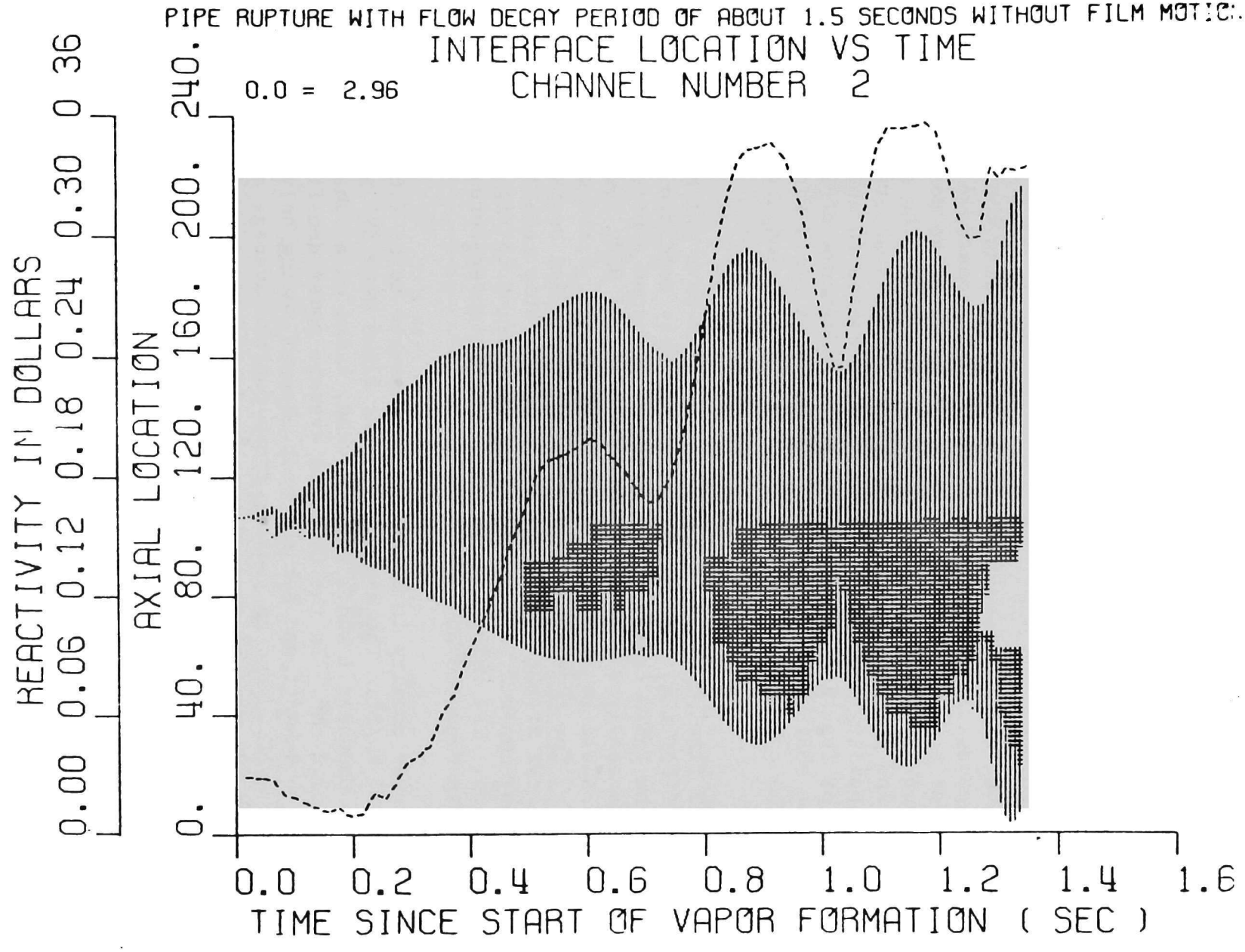

Fig. 11. Sodium Liquid-vapor Interface Location for 1.5 sec Pipe Rupture Accident, Static Film, 1-phase Friction Factor. ANL Neg. No. 116-76-13.

C. More Extreme Pipe Rupture Accidents

The purpose of this series of calculations was to study conditions arising with extremely rapid flow decay, such as might occur with a double-ended pipe rupture at the reactor coolant inlet nozzle. In order to achieve an extremely rapid flow reduction in SAS it was found necessary to use a tabular input of $\Delta P/\Delta P_o$, the ratio of the pump head to the steady-state value, as a function of time. $\Delta P/\Delta P_o$ was unity until t = 0.004 sec, and then held constant at various final values ranging from 0.01 to 0.1. These ratios labeled simply ΔP, by which they will be referred to henceforth, appear as parameters in Fig. 12, which shows the corresponding rate of flow reduction obtained as a function of time, and in Fig. 13 and 14.

In cases without scram it was found that sodium boiling would not occur until about 1.3 seconds regardless of the rate of flow coastdown simply because of the heat transfer time constants involved. There was also not much sensitivity to steady-state power-to-flow ratio. This time was extended to about 1.5 seconds for ΔP up to 0.05 and to 2-3 seconds for $\Delta P = 0.10$. The reactor power stayed near normal until boiling occurred, and actually decreased to about 0.8 of normal in the slower of the flow decays considered here because of a negative effect of expansion of hot sodium above the core. In the most rapid flow decays the heat capacity of the upper blanket kept the sodium cooler and the power stayed at normal.

The very rapid flow coastdown cases without scram have not been pursued beyond the start of boiling. If they were, disassembly conditions similar to those of Table V and Table IX should be obtained. Because a massive pipe rupture accident is generally regarded as being an event of very low probability, it seems most reasonable to assume that, if it did occur, scram would be operative. Accordingly, for $\Delta P = 0.02$ and $\Delta P = 0.03$, scram was assumed effective at about 0.6 sec after attainment of a power to flow ratio relative to steady state of 1.15 in any channel, a condition which according to Fig. 11 was attained in 0.01-0.02 seconds. The resulting fuel and sodium temperatures was a function of time are shown in Figs. 13 and 14.

The average power density in Channel 1 was assumed to be 8.6 kw/ft and in Channel 2 it was 9.1 kw/ft. The assumed coolant flows were 592 gms/cm^2 and 731 gms/cm^2-sec in Channels 1 and 2 respectively, based on a subassembly cross sectional area of 37.2 cm^2. In the CRBR the average power density for the average channel is 6.6 kw/ft and for the peak channel, using only nuclear peaking factors, it is 9.1 kw/ft. Design coolant flows for the average and hottest channel are 568 and 626 gms/cm^2-sec. Our assumed conditions were thus slightly less severe than for the CRBR peak channel, excluding engineering hot channel and flow maldistribution factors.[1] When these factors are included, the transient condition in a CRBR pipe rupture becomes considerably more severe than we have assumed. Boiling would clearly occur in the CRBR for the fractional final flow rates we have considered here when these hot channel factors are applied.

It appears that in our model a boiling temperature of 990°C, including 10° superheat, would be attained in the $\Delta P = 0.02$ case (final flow 7% of original) but not in the $\Delta P = 0.03$ case (final flow 11% of original). Actually the outlet pressure in these calculations of 2.1 atm may be too high, and a boiling temperature of 950°C, about what was attained in the $\Delta P = 0.03$ case, is probably more appropriate. Although the final fractional flow of 6.6% in the $\Delta P = 0.02$

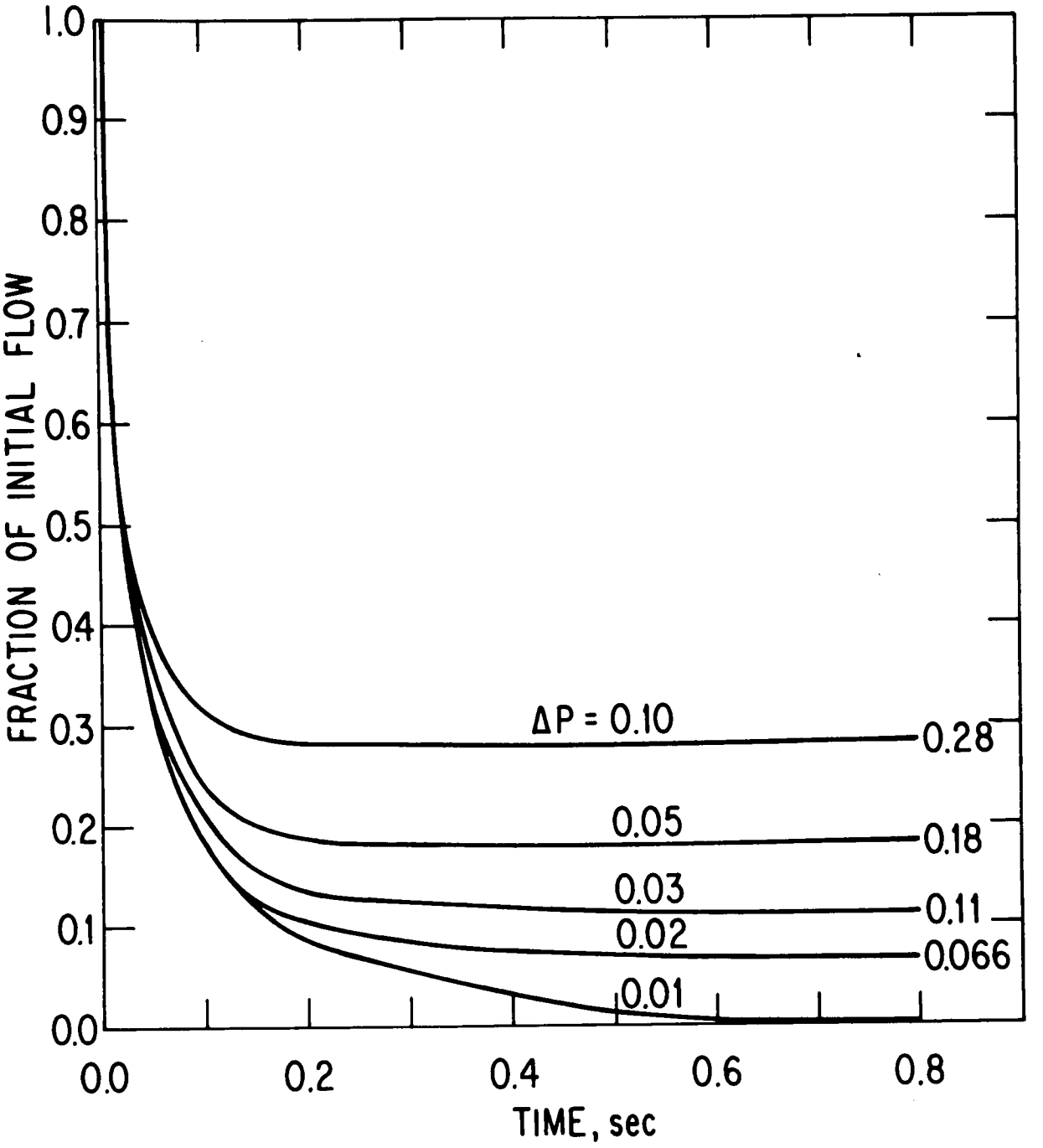

Fig. 12. Fractional Flow Reduction Rates for Extreme Pipe Rupture Accidents. ANL Neg. No. 116-76-19.

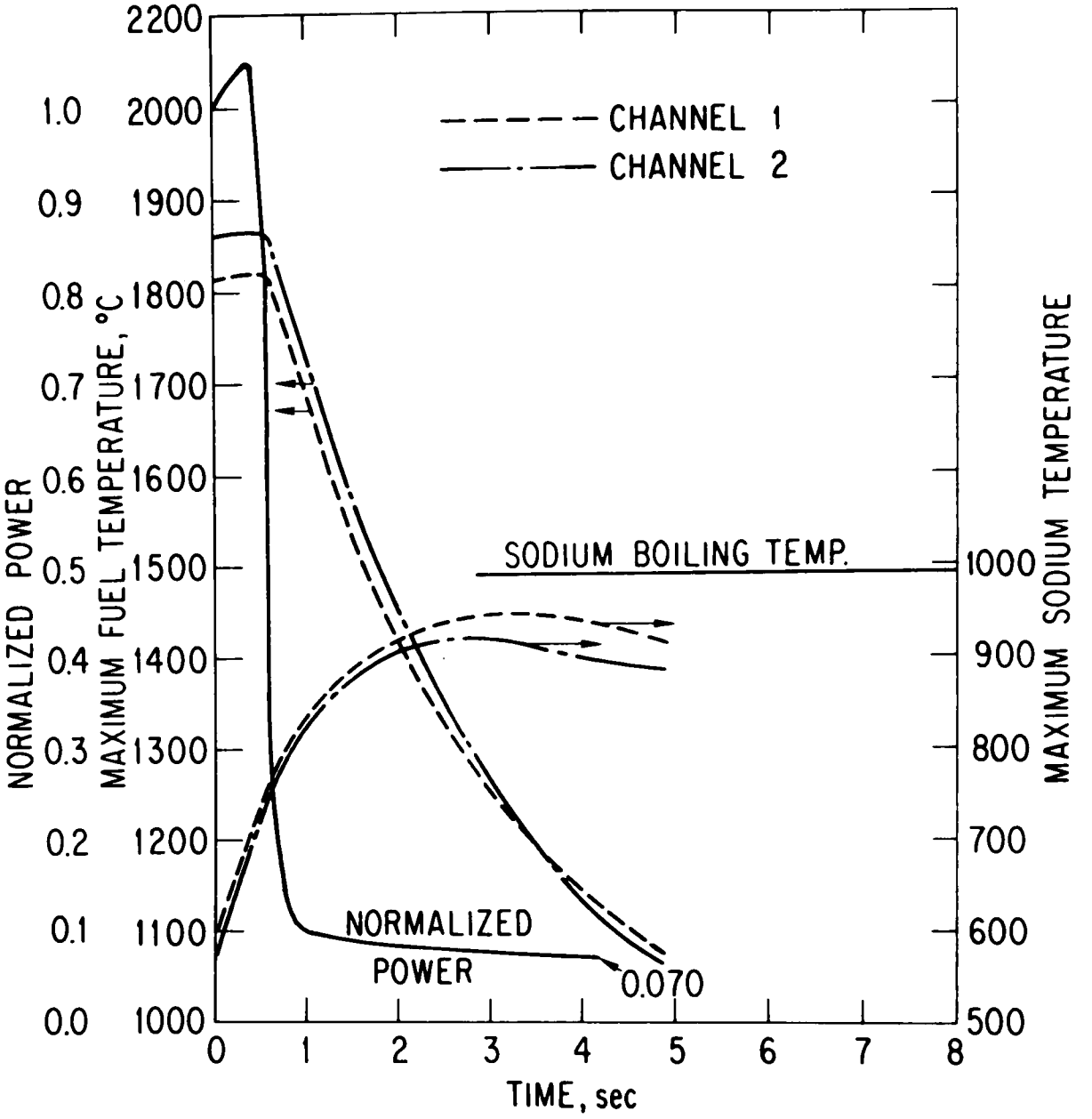

Fig. 13. Results for Extreme Pipe Rupture Accident with Scram, $\Delta P = 0.02$.
ANL Neg. No. 116-76-8.

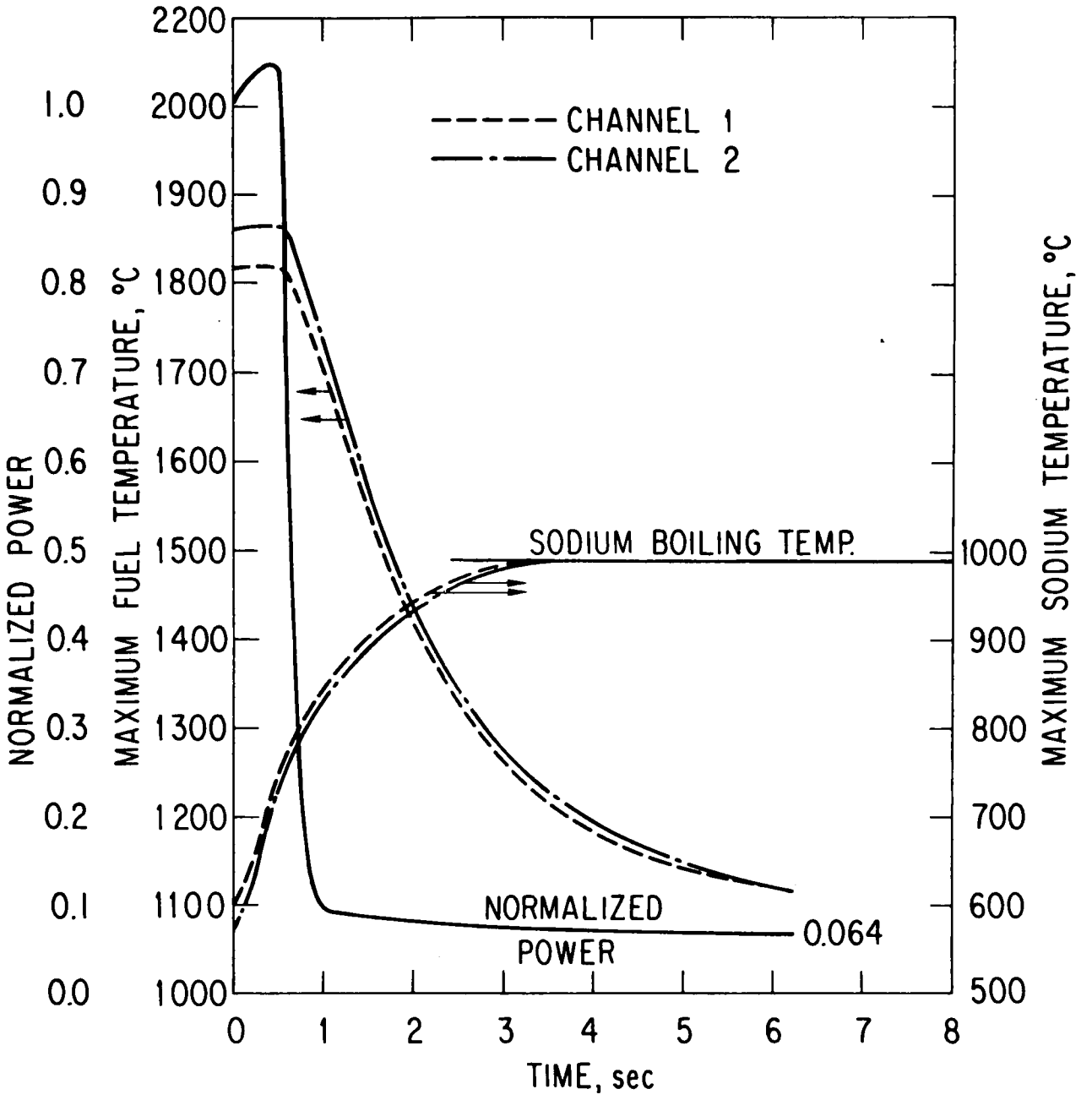

Fig. 14. Results for Extreme Pipe Rupture Accident with Scram, $\Delta P = 0.03$.
ANL Neg. No. 116-76-21.

case about balances the decay heat power of 6.4% of normal attained after several seconds, the effect of the heat stored in the pin causes overheating of the coolant to occur.

Besides the pin power density and coolant flow rate, an important factor affecting LOF boiling conditions for a gas-bonded pin is the fuel-clad gap conductance, which affects the heat stored in the pin and the rate at which heat is transferred to the coolant under transient conditions.[19] In our calculations the gap conductance was about 1.0 watt/cm^2-°C. This conductance is sensitive to burnup because of the effect both on gap widths and on bond gas composition: conductivity is much lower for fission gas than for He. While it is hard to tell in practice what the right combination of gap width and bond gas composition is for irradiated fuel, a conductance of about 0.4 seems to be a reasonable lower bound in the light of the LIFE-II correlation[20] and of results from the water-reactor program.[21] We have evaluated the effect of a decrease in gap conductance to 0.4 watt/cm^2-°C and found that in this case boiling occurred for $\Delta P = 0.05$ (final flow 18% of the original), but did not for $\Delta P = 0.10$ (final flow 28% of original). Evaluation of gap conductance thus seems to represent a large uncertainty in determining what flow rate is needed to prevent coolant boiling in a pipe rupture accident.

VII. CONCLUSIONS

The feedback mechanisms we have considered do not lead to violent initial disassembly regardless of assumption made about clad motion, axial fuel expansion, or flow coastdown rate. Considerable variations in feedback coefficients can occur without important effects on accident severity because of compensating changes that tend to take place, provided there is not a large change in reactivity ramp rate and that a reasonable prompt negative feedback is present. In particular, burnup effects do not seem to be of crucial importance in increasing accident severity. Even milder disassemblies than we have calculated are possible if fuel sweepout by sodium liquid or vapor or by fission gas could occur. A crude evaluation of the effect of the LOF-driven TOP, which cannot be treated adequately by SAS-3A, indicates that in the CRBR it might cause a moderate increase in accident severity. Fuel slumping and sodium voiding reactivity ramp rates tend to be smaller than those from clad motion as calculated by CLAZAS, but the total ramp rate in the absence of a LOF-driven TOP does not exceed $40/sec. Substantially higher ramp rates than those found here are conceivable but the assumptions needed to obtain them tend to be rather farfetched.

Study of very rapid flow decay transients presumed to result from double-ended pipe ruptures indicates considerable sensitivity of boiling conditions to fuel pin power density and fuel-clad gap conductance. For the hottest channel of the CRBR, taking into account engineering hot channel factors, flows for several seconds after the rupture greater than 25% of the initial flow appear to be needed to prevent boiling.

APPENDIX

PARAMETER STUDIES WITH PLUTO TO ESTIMATE RAMP RATES IN A LOF-DRIVEN TOP

Results of parameter studies with PLUTO for an assumed central figure are given in Table A1. In this Table "B" refers to the base case, which is the first one listed. Blank entries in the table imply that the appropriate value is the nearest non-blank entry above. Results are given in terms of molten fuel expelled per pin and sodium reactivity change per subassembly at 10 and 50 milliseconds after pin failure. It was felt that because of uncertainty in fuel motion in the channel, considering that PLUTO does not account for fuel freezing, the total fuel expelled from the pin is more significant as it gives a measure of the total reactivity effect that would occur if fuel expelled from the pin remained at the point of clad failure, a conservative assumption. The significance of the fuel mass expelled can be understood by noting that 13 gms of fuel expelled from the center of a pin in CRBR subassembly Ring 8 and not moving in the channel corresponds to about $0.01 per subassembly; the corresponding values for Ring 7 and Ring 9 are $0.007 and $0.0085. These values together with the coherence of failure assumed above lead to a fuel-motion ramp rate of $50/sec over 10 milliseconds. Although 13 gms fuel expulsion in 10 milliseconds is not the largest value in the table, it appeared to be sufficiently conservative in view of the assumption of central failure and of no fuel motion in the channel.

TABLE A1. PLUTO Results - Failure at Core Center

Case	Gms Fission Gas/gm Fuel $\times 10^3$	Particle Radius, cm	Fuel Thermal Conductivity	Cavity Radius, cm	Cavity Temp., °K	Channel Fuel Mass Per Pin		Na Reactivity per Subassembly $\delta k \times 10^5$ (CRBR Ring 8)	
						10 ms	50 ms	10 ms	50 ms
Base	0.229	0.025	B	0.2543	3125	13.30	29.16	0.980	2.048
1					3500	13.67	31.10	1.061	1.990
2					4000	13.96	33.40	1.166	1.929
3	B	0.010	B	B	B	4.97	30.82	1.568	1.364
4		0.025				13.30	29.16	0.980	2.048
5		0.050				14.78	30.44	0.917	2.281
6	0.100	B	0	B	B	10.60	22.71	0.536	1.115
7	0.229					15.05	34.64	0.903	1.977
8	0.500					19.64	44.13	1.353	2.059
9	0.1	0.01	B	B	B	2.78	18.03	1.069	1.621
10	B	B	B	0.2	B	9.54	19.24	0.785	2.129
11	0.500	B	B	B	B	18.53	40.35	1.423	1.883
12	B	0.050 (10 ms, 0.010)	B	B	B	14.78	28.38	0.917	1.373

NOTE: "B," base case.

For sodium reactivity, the positive effect in Ring 8 is about cancelled by a negative effect in Ring 9. For Ring 7 voiding the worth per subassembly for the first 10 milliseconds is about 2.3 times that in Ring 8, which for 24 subassemblies leads to a void worth of about $2.3 \times 1.3 \times 10^{-5}$ k × 24 or ∿\$0.25 and a ramp rate for the first 10 milliseconds of ∿\$25/sec.

It is seen (Cases "B," 1, 2) that change in cavity temperature over a reasonable range has little effect on reactivity as the fission-gas pressure does not change much. Note that fuel vapor pressure is not taken into account, and at 4000°K becomes comparable to the fission-gas pressure 10 to 20 milliseconds after pin failure. The effect of cavity temperature cannot really be calculated satisfactorily above about 3700 or 3800°K without putting in fuel vapor effects.

In the next set of calculations (Cases 3, 4, 5), the strength of the fuel-coolant interaction (FCI) has been varied by varying the fuel-particle radius, to which the heat transfer coefficient between fuel and coolant is assumed inversely proportional in the steady-state Cho-Wright formalism assumed here. In the last line of the table (Case 12) the particle radius is set initially at 0.050 cm and after 10 milliseconds is assumed to decrease by fragmentation to 0.010 cm. A strong FCI is seen to delay the ejection of fuel from the pin, and to increase the sodium reactivity somewhat. The sodium reactivity is less at 50 milliseconds with a strong FCI because more voiding in regions of negative void worth occurs.

The next group of calculations (Cases 6, 7, 8) explores the effect of varying fission gas content over what seems to be a reasonable range for irradiated fuel on the basis of SAS-3A calculations. The FCI has been eliminated in these cases by setting the fuel conductivity equal to zero. Comparison of the second of these cases with the base case shows that the base case FCI is too weak to have much effect compared to the effect of fission gas. The sodium-voiding reactivity is low for a gas content of 0.1×10^{-3} because with the FCI cut off little voiding of sodium occurs.

REFERENCES

1. *Preliminary Safety Analysis Report*, Clinch River Breeder Reactor Project, Project Management Corp., Oak Ridge, Tennessee.

2. M. G. Stevenson, et al, *Current Status and Experimental Basis of the SAS LMFBR Accident Analysis Code*, Proc. Fast Reactor Safety Meeting, April 2-4, 1974, Beverly Hills, Calif., CONF-740401-P3, pp. 1303-1321.

3. B. J. Toppel, *The New Multigroup Cross Section Code MC^2-2*, Proceedings of Conference on New Developments in Reactor Mathematics and Applications, CONF-710307 (1971).

4. W. M. Stacey, Jr., et al, *Studies of Methods for Fast Neutron Multigroup Cross Section Generation and Their Effect Upon the Neutronics Properties of LMFBR Critical Assemblies*, CONF-720901 (1972).

5. Kalimullah, *CRBR Equilibrium Cycle Calculations Using the REBUS Code*, in Physics of Reactor Safety, Quarterly Report for January-March 1975, ANL-75-31, p. 10.

6. F. E. Dunn, et al, *The SAS-3A LMFBR Accident Analysis Computer Code*, ANL/RAS 75-17, April 1975.

7. W. R. Bohl, *SLUMPY: The SAS-3A Fuel Motion Model for Loss-of-Flow*, ANL/RAS 74-18, August 1974.

8. W. R. Bohl and T. J. Heames, *CLAZAS: The SAS-3A Clad Motion Model*, ANL/RAS 74-15, August 1974.

9. L. L. Smith, *SAS-FCI, A Fuel-Coolant Interaction Model for LMFBR Whole-Core Accident Analysis*, ANL/RAS report, to be issued.

10. G. Höppner, *Sodium Film Motion Model of SAS-3A*, ANL/RAS report, to be issued.

11. F. E. Dunn, J. Travis, and L. L. Smith, *The PRIMAR-II Primary Loop Hydraulics Routine in the SAS-3A Code*, ANL/RAS report, to be issued.

12. H. U. Wider, et al, *An Improved Analysis of Fuel Motion During LMFBR Overpower Excursion Using a New Model*, Ibid Ref. 2, p. 1550.

13. H. K. Fauske, *Some Comments on Cladding and Early Fuel Relocation in LMFBR Core Disruptive Accidents*, Trans. Am. Nucl. Soc. 21, 322 (1975).

14. H. H. Hummel and C. N. Kelber, *Realistic Upper Bounds for Reactivity Insertion from Slumping Fuel*, Proceedings of Conference on Mathematical Models and Computational Techniques for Analysis of Nuclear Systems, Ann Arbor, Michigan, April 9-11, 1973, CONF-730414-P2, pp. V-125 to V-136.

15. H. U. Wider, private communication.

16. *Preliminary Safety Analysis Report*, Clinch River Breeder Reactor Project, Appendix F, Amendments, Project Management Corp., Oak Ridge, Tennessee, October 1975.

17. G. Höppner, private communication.

18. W. R. Bohl, private communication.

19. K. Miles and I. T. Hwang, private communication.

20. V. Z. Jankus and R. W. Weeks, *LIFE-II, A Computer Analysis of Fast-Reactor Fuel-Element Behavior as a Function of Reactor Operating History*, Nuclear Engineering and Design, Vol. 18, No. 1, January 1972, pp. 83-96.

21. D. D. Lanning, C. R. Hann, and E. S. Gilbert, *Statistical Analysis and Modeling of Gap Conductance Data for Reactor Fuel Rods Containing UO_2 Pellets*, BNWL-1832, August 1974.